AARHUS-ASTRO-1993-5

Nordic Optical Telescope Imaging of the Gravitational Lens Candidate QSO 1208+1011*

Jens Hjorth† and Frank Grundahl Jensen†

Institute of Physics and Astronomy, Aarhus University, DK-8000 Århus C, Denmark

Abstract: We present high-resolution optical images of the recently discovered gravitational lens candidate QSO 1208+1011. The small image separation of 0.″48 between its two components makes it a challenging object for ground-based photometry. By resampling, registration, and combination of the obtained images we demonstrate that physical parameters for the system can be derived using maximum entropy deconvolution and detailed point source photometry. Reductions of simulated images and comparison with Hubble Space Telescope (HST) data indicate the reliability of these results and suggests that accurate ground-based photometry can be performed even for gravitational lens systems with very small image separations.

1 Introduction

QSO 1208+1011 is a newly discovered gravitational lens candidate. In 1986 it represented the most distant known quasar [HAZ86.1], [SAR86.1] and was found in 1991 to consist of two images [MAG92.1], [MAO92.2]. Hubble Space Telescope (HST) imagery [BAH92.3] and spectroscopy [BAH92.1], which show that the spectra of the two components are very similar, indicate that this effect could be attributed to gravitational lensing of a single quasar by a foreground galaxy. As such QSO 1208+1011 is one of the most distant gravitational lens candidates ($z = 3.8$) with one of the smallest separations between its two components (0.″48). However, the lensing galaxy has not been detected.

On June 22 1992 we obtained 5 frames in the visual filter, V, and 5 frames in the red filter, R, of this quasar with the Nordic Optical Telescope (NOT) on La Palma equipped with the stand-by Stockholm CCD camera which has 0.″2/pixel. Stellar images had a FWHM of 0.″55 to 0.″65, but were affected by triangular astigmatism due to malfunction of the supports of the secondary mirror at the time of observation. In Fig. 1a is shown one such image of the quasar.

We have used these data for a pilot study aimed at probing the limits of what can be achieved from the ground given the limitations set by the unavoidable atmospheric blurring and finite detector pixel size. QSO 1208+1011 is an excellent target for this purpose because of the small image separation and the relatively large pixel size of the CCD used.

*Based on observations obtained at the Nordic Optical Telescope, La Palma

†Electronic mail addresses: jens@obs.aau.dk, fgj@obs.aau.dk

We here present preliminary results of our experiments on resampling, image combination, image restoration, and photometry. The quest for optimal procedures for such tasks is important for CCD photometry in general and for crowded field photometry and photometry of sparsely sampled images (e.g., Stockholm CCD, IR arrays, HST images) in particular.

2 Preprocessing

Individual images were bias subtracted, non-linearity corrected, dark corrected, and flat fielded using dome flats.

Finally, two coadded images were constructed as follows. The telescope had been shifted between exposures implying that each image was sampled in different ways by the CCD detector. To take advantage of this extra information present in the data we resampled each pixel into 5×5 pixels and subsequently shifted the images integral pixels to a common coordinate system. The bilinear interpolation used in this procedure introduced some spiky artifacts at the old pixel borderlines, but these were essentially averaged out through the final combination of 5 images into one (for each filter). Our final combined images consist of a 1000 sec R frame and a 1300 sec V frame with an angular resolution of 0.″65 FWHM and sampled with 0.″04/pixel. They are thus adequately sampled for the subsequent deconvolution and photometry. In Fig. 1b the combined R image is shown.

3 Maximum Entropy Deconvolution

We have developed a code for deconvolution of images and spectra based on the Maximum Entropy Method (MEM, cf. [NAR86.1]) described by [ALH78.1] and [HOL92.1]. Provided the PSF is space invariant the iterative procedure and the convolutions and cross-correlations are easily implemented numerically using Fast Fourier Transforms (FFTs). With only 4 FFTs per iteration this method is as fast as the popular Richardson-Lucy technique [LUC74.1]. The code has been implemented in Interactive Data Language (IDL) which allows graphical monitoring of the deconvolution in real time. This option is very useful since some experimenting is often required to obtain reliable results.

The point spread function (PSF) was determined from a star 20″ North of the quasar, comparable in magnitude to the quasar. The (sky subtracted) noisy outer parts of the PSF was set to zero and the outer regions of the quasar were masked out. The essential inner regions were unaffected.

The algorithm was then run for 1000 iterations. In most applications much fewer iterations is normally employed, but to obtain a large gain in resolution a large number of iterations is required. The results show that no artifacts are produced: In Fig. 1c is shown the two components (A and B; A is the bright Northern component) of the quasar after deconvolution The FWHM is 0.″15, i.e., an improvement of a factor 4 in resolution. For an impression of the gain in resolution, see also Fig. 2. For comparison is shown a Planetary Camera picture from HST [BAH92.3] in Fig. 1d. We find that the two quasar images from NOT have identical positions in the two colours and that they are fully compatible with the HST results. In addition, they have the correct intensity ratio (4:1). This is intriguing since MEM is normally believed to be photometrically unreliable.

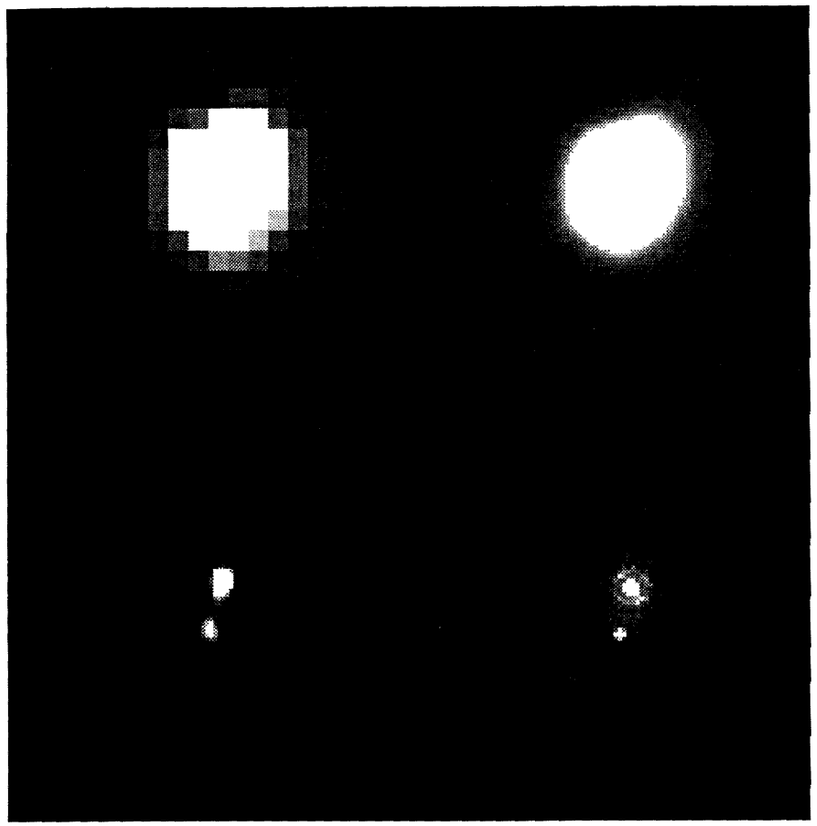

Figure 1: Images of QSO 1208+1011 taken through a red filter. The four images are 4″× 4″ each. North is up and East is to the left. *Upper left (a)*: Single 300 sec R exposure from NOT. The sampling is 0.″2/pixel and the FWHM ≈ 3 pixels. *Upper right (b)*: Combination of 5 resampled R exposures from NOT. The total exposure time is 1000 sec, the sampling is 0.″04/pixel, and the FWHM ≈ 15 pixels. *Lower left (c)*: Combined image shown upper right after 1000 MEM iterations. The FWHM is approximately 4 pixels. *Lower right (d)*: Image obtained with WFPC/HST. The filter is F702W, the total exposure time is 600 sec, and the sampling is 0.″044/pixel.

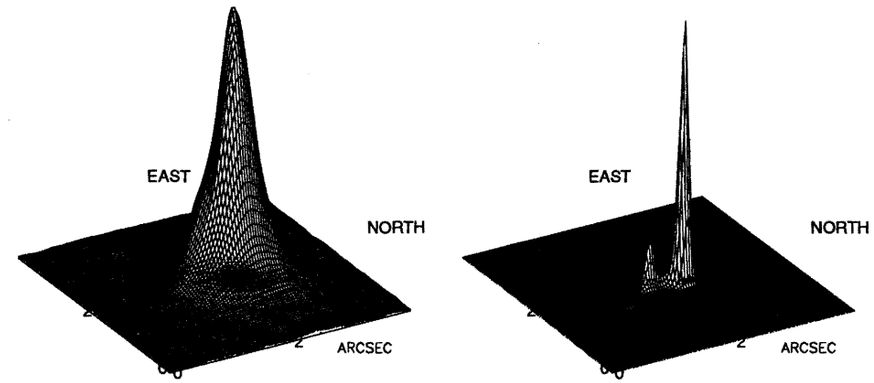

Figure 2: QSO 1208+1011 before (*left*) and after (*right*) deconvolution with 1000 MEM iterations.

4 Photometry

The result of the MEM deconvolution (i.e., knowledge of approximate positions and magnitudes) can be used as input for the point source photometry package DAOPHOT/ALLSTAR [STE87.1] developed for crowded field photometry. ALLSTAR performs simultaneous least squares profile fitting to all objects in a given frame. In our case the model of the stellar profile (PSF) was derived from the same star as used for the MEM deconvolution. The profile fitting is done by an iterative procedure and gives the (x, y) position and brightness of an object. The photometry was performed on images resampled to 0.″08/pixel.

In order to assess the reliability of our photometry on resampled images we have created three sets of simulated data (sim1–3) including the PSF star and the double quasar image. Each set of images consists of 5 'R exposures' of 200 sec each. Photon and read noise were included and the PSF used was very similar to the real PSF, but had a slightly lower resolution. The simulated images were resampled, shifted and combined in a manner identical to the real images. 'True' parameters of the three final images are given in Table 2 ('angle' refers to the angle between AB and up–down).

The three combined simulated images, although they look very much alike, behave quite differently in response to varying DAOPHOT parameters. After convergence several parameters describing the quality of the fit are provided: We have focused on the SHARP parameter which is a measure of how well the width of the object matches that of the model PSF. For resolved galaxies SHARP will be significantly greater than zero whereas for cosmic ray events it will be somewhat smaller than zero.

We have found that in general an optimal fit can be obtained by minimizing the magnitude of the SHARP parameter by varying the FITTING RADIUS (FRAD) of the PSF fitting routine ALLSTAR provided that a number of DAOPHOT parameters are suitably chosen. From an exploration of the vast parameter space of DAOPHOT we arrived at the parameters given in Table 1—it must be stressed, however, that these preliminary results are specific for the

Table 1: DAOPHOT/ALLSTAR parameters used for photometry on QSO 1208+1011.

DAOPHOT	
PSF RADIUS	15
ANALYTIC PSF	2
FITTING RADIUS	2
VARIABLE PSF	0

ALLSTAR	
CLIPPING EXPONENT	1
INNER SKY	25
OUTER SKY	35

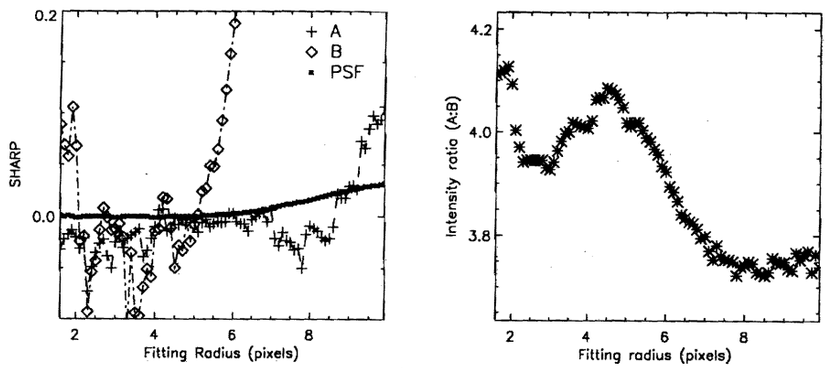

Figure 3: (*a*) SHARP and (*b*) the intensity ratio A:B as a function of FRAD for the simulated image sim1. The optimal choice of FRAD is found from (*a*) to be FRAD=5.1 yielding A:B=4.01 cf. (*b*) and Table 3.

problem in hand and cannot in general be considered optimal.

With these parameters fixed we then varied FRAD of ALLSTAR. We show an example in Fig. 3 for one of the simulated images (sim1). In Table 2 are given the results when SHARP is minimized. Two of the simulations yield impressive results, whereas one gives a too low value for the intensity ratio A:B. However, this image (sim2) can be discerned by the A–PSF distance which is slightly too low.

The multiple fit of DAOPHOT has enabled us to derive very precise parameters for the observed system. Raw parameters are given in Table 2. The physical parameters are given in Table 3 where the first three entries refer to the intensity ratios between the two components, the angle with respect to the NS direction, and the separation between the two components. The A:B uncertainty has been estimated to be slightly lower than indicated in Table 2 since the two A–PSF distances agree very well; in fact we believe that it is likely that the stated results may be very close to the true values, i.e., with an uncertainty of less than ±0.05. The physical angles and separations are derived from knowledge of orientation and scale of the CCD (e.g., [VES92.1])—this transformation gives a major contribution to the uncertainties in Table 3.

Using standard stars from the globular cluster M92 [CHR85.1] and mean values for the extinction at La Palma we arrive at the photometry given in Table 3. In Table 3 are also shown the corresponding HST data [BAH92.3], [MAO93.2]. It is evident that our ground-based photometry is fully compatible with the space-based observations.

Table 2: True and inferred parameters for simulated and real images of QSO 1208+1011

Image	FRAD	A:B	Angle (°)	Separation (px)
sim1	5.1	4.01	15.6	6.07
sim2	5.4	3.62	14.5	5.91
sim3	5.7	4.01	14.6	5.97
Inferred		3.9±0.2	14.9±0.7	5.98±0.09
True		4.00	15.0	6.00
V	5.7	4.15	13.4	5.98
R	5.2	3.93	13.8	5.93

Table 3: NOT and HST physical parameters for QSO 1208+1011.

NOT[a]	V	R
A:B	4.15 ± 0.15	3.95 ± 0.15
Angle	$14.9° \pm 1°$	$15.3° \pm 1°$
Separation	$0''.474 \pm 0''.008$	$0''.470 \pm 0''.008$
QSO magnitude	17.91 ± 0.07	17.38 ± 0.07
PSF magnitude	18.51 ± 0.07	18.15 ± 0.07

HST[b]	V (F555W)	R (F702W)
A:B	4.2 ± 0.1	4.0±0.1
Angle	15°	
Separation	$0''.476 \pm 0''.004$	
QSO magnitude	17.9 ± 0.1	
PSF magnitude	18.5 ± 0.1	

[a] June 22 1992

[b] December 23 1991 (F555W) and January 20 1992 (F555W and F702W) [BAH92.3]

5 Discussion and Conclusions

QSO 1208+1011 has a strong Ly α/N v emission line at around 5900 Å. This is just inside the V band and outside the R band we used. The fact that the intensity ratios between A and B are almost identical in these filters strongly supports the gravitational lens hypothesis. However, the intensity ratio is marginally larger in V than in R both in our data and in the HST data and thus appears significant. The data also indicate that the brightness of the quasar did not change significantly during the first half of 1992.

In conclusion, we have presented preliminary results from a study of a small-separation gravitational lens candidate. The main results are summed up in Fig. 1 and Table 3. We have demonstrated that useful images can be created through resampling and registration of several frames. MEM deconvolution yields a gain of a factor 4 in resolution (FWHM less than the original pixel size) and appears to be photometrically reliable, at least in this 'simple' system.

The method appears promising for performing accurate photometry on this and other closely spaced gravitational lenses, e.g., B0218+357 [PAT92.1] and BRI0952–01 [MCM92.1], and thus to monitor for microlensing and time delays. The technique may also be useful for narrow

band imagery of gravitational lens candidates for which spectroscopy is difficult or impossible to obtain; this could be the case in systems like B1422+2309 [PAT92.2], [LAW92.1].

Acknowledgements

We thank the NOT staff for invaluable help during observations and Peter Stetson for advice on DAOPHOT parameters. The project was supported by the Danish Board for Astronomical Research. JH acknowledges support from the Carlsberg Foundation.

References

[ALH78.1] Alhassid, Y., Agmon, N., Levine, R. D.: 1978, *Chem. Phys. Lett.* **53**, 22

[BAH92.3] Bahcall, J. N., Maoz, D., Schneider, D. P., Yanny, B., Doxsey, R.: 1992, *ApJ* **392**, L1

[BAH92.1] Bahcall, J. N., Hartig, G. F., Jannuzi, B. T., Maoz, D., Schneider, D. P.: 1992, *ApJ* **400**, L51

[CHR85.1] Christian, C. A., Adams, M., Barnes, J. V., Butcher, H., Hayes, D. S., Mould, J. R., Siegel, M.: 1985, *PASP* **95**, 439

[HAZ86.1] Hazard, C., McMahon R. G., Sargent, W. L. W.: 1986, *Nature* **322**, 38

[HOL92.1] Hollis, J. M., Dorband, J. E., Yusef-Zadeh, F.: 1992, *ApJ* **386**, 293

[LAW92.1] Lawrence, C. R., Neugebauer, G., Weir, N., Matthews, K., Patnaik, A. R.: 1992, *MNRAS* **259**, 5P

[LUC74.1] Lucy, L. B.: 1974, *AJ* **79**, 745

[MCM92.1] McMahon, R., Irwin, M., Hazard, C.: 1992, *Gemini Newsletter* **36**, 3

[MAG92.1] Magain, P., Surdej, J., Vanderriest, C., Pirenne, B., Hutsemékers, D.: 1992, *A&A* **253**, L13

[MAO92.2] Maoz, D., Bahcall, J. N., Schneider, D. P., Doxsey, R., Bahcall, N. A., Filippenko, A. V., Goss, W. M., Lahav, O., Yanny, B.: 1992, *ApJ* **386**, L1

[MAO93.2] Maoz, D., Bahcall, J. N., Schneider, D. P., Bahcall, N. A., Djorgovski, S., Doxsey, R., Gould, A., Kirhakos, S., Meylan, G., Yanny, B.: 1993, *ApJ* **409**, 28

[NAR86.1] Narayan, R., Nityananda, R.: 1986, *ARA&A* **24**, 127

[PAT92.2] Patnaik, A. R., Browne, W. A., Walsh, D., Chaffee, F. H., Foltz, C. B.: 1992, *MNRAS* **259**, 1P

[PAT92.1] Patnaik, A. R., Browne, W. A., King, L. J., Muxlow, T. W. B., Walsh, D., Wilkinson, P. N.: 1993, *MNRAS* **261**, 435

[SAR86.1] Sargent, W. L. W., Filippenko, A. V., Steidel, C. C., Hazard, C., McMahon, R. G.: 1986, *Nature* **322**, 40

[STE87.1] Stetson, P. B.: 1987, *PASP* **99**, 191

[VES92.1] Vestergaard, M., Barthel, P. D.: 1992, *NOT News* **6**, 32